energies

MDPI

Communication

Effect of Salt Concentration, Solvent Donor Number and Coordination Structure on the Variation of the Li/Li$^+$ Potential in Aprotic Electrolytes

P. K. R. Kottam, S. Dongmo, M. Wohlfahrt-Mehrens and M. Marinaro *

ZSW—Zentrum für Sonnenenergie und Wasserstoff-Forschung Baden-Württemberg, 89081 Ulm, Germany; pranay.kottam@zsw-bw.de (P.K.R.K.); saustin.dongmo@zsw-bw.de (S.D.); margret.wohlfahrt-mehrens@zsw-bw.de (M.W.-M.)

* Correspondence: mario.marinaro@zsw-bw.de

Received: 20 February 2020; Accepted: 17 March 2020; Published: 20 March 2020

Abstract: The use of concentrated aprotic electrolytes in lithium batteries provides numerous potential applications, including the use of high-voltage cathodes and Li-metal anodes. In this paper, we aim at understanding the effect of salt concentration on the variation of the Li/Li$^+$ Quasi-Reference Electrode (QRE) potential in Tetraglyme (TG)-based electrolytes. Comparing the obtained results to those achieved using Dimethyl sulfoxide DMSO-based electrolytes, we are now able to take a step forward and understand how the effect of solvent coordination and its donor number (DN) is attributed to the Li-QRE potential shift. Using a revised Nernst equation, the alteration of the Li redox potential with salt concentration was determined accurately. It is found that, in TG, the Li-QRE shift follows a different trend than in DMSO owing to the lower DN and expected shorter lifespan of the solvated cation complex.

Keywords: lithium; reference electrode; high concentrated electrolytes; ferrocene; Nernst equation; cyclic voltammetry; donor number

1. Introduction

Li-ion batteries (LIBs) are undeniably the current world leader in solving energy storage problems. For LIB cells, electrolytes based on carbonates solvents are state-of-the-art materials. However, these electrolytes possess a relatively low electrochemical stability window that limits their use for both next generation 5V cathodes and Li metal anodes [1]. Recent reports on the use of concentrated solutions as electrolytes for future Li batteries have been on the rise [2,3]. The presence of a near zero free solvent concentration at these high concentrations favours its stability against solvent decomposition. We previously investigated the effect of Li-salt concentration on the variation of the Li-QRE potential in DMSO-based electrolytes [4]. Based on our previous results, the trend in the potential shift is more pronounced at high salt concentrations owing to the change in the coordination structure of Li$^+$ ions. Such a similar shift in the potential trend has also been reported by Ernould et. al., in ethylene carbonate (EC): diethyl carbonate (DEC): Tri-ethyl phosphate (TEP) mixtures, wherein they observed a maximum shift of -500 mV with increasing organic phosphate concentration [5]. In addition, a variation in solvent also affects the shift of the Li-redox potential, revealing the solvent-dependence of the Li-solvation free energy [6]. For example, a relatively high donor number (DN) solvent more readily solvates the Li$^+$ ions than solvents with lower DN. However, there are only a few studies reporting on the variation of the Li- Quasi-Reference Electrode (QRE) potential shift as a function of both salt concentration and solvent DN. In this prospect, we chose Tetraglyme (TG) solvent, which possesses a low DN (12 kcal/mol) [7], and compared it to the previously investigated Dimethyl sulfoxide (DMSO; DN = 29.9 kcal/mol) [8] to

specifically address the effect of the DN. These two aforementioned solvents are quite commonly used in post Li-ion battery cells (i.e., Li-O_2) [3,9–16]. Using a concentration cell setup, the electromotive force (EMF) is measured with respect to various salt concentrations. Furthermore, the obtained results are validated using a standard internal reference system, namely ferrocene (Fc), as the Fc/Fc^+ couple is reportedly stable under salt and solvent variation [4,17]. We believe that the dependency of Li-QRE potential on (1) solvent DN and (2) Li-ion concentration in aprotic electrolytes is scarcely investigated and little-understood. Our study aims to shed some light on such phenomena. Moreover, in agreement with Mozhzhukhina and Calvo [17], our current study stresses the necessity of specifying the solvent, electrolyte salt and Li^+ concentration when performing an electrochemical measurement using lithium metal as the reference electrode.

2. Materials and Methods

Lithium-Bis(trifluoromethane)sulfonimide (LiTFSI) purchased from Solvionic (99.9% pure) was dried in a Büchi oven at 140 °C for 72 h under vacuum. TG purchased from Sigma-Aldrich (>99.9% pure) was dried with pre-treated molecular sieves (4 Å) in accordance with our previously reported studies [4]. Additionally, ferrocene (Fc) purchased from Sigma-Aldrich (99% pure) was dried overnight in the Büchi oven at 150 °C. Finally, 0.05, 0.2, 1,2 and 3 M LiTFSI/TG solutions were prepared with 7.5 mM Fc and stored in a glovebox with O_2 and H_2O levels below 0.1 ppm. A three-electrode beaker cell setup was used to collect the cyclic voltammograms for different concentrations. An Au disk (PINE E6 standard) was used as working electrode and polished before and after each measurement with fine grinding papers. The polished and cleaned electrode was then dried at 120 °C under vacuum in a Büchi oven for 24 h before the next experiment. Lithium metal strips (Alfa Aesar; 99.9% pure; 0.03-inch thickness) acted as counter and reference electrodes. Raman spectroscopy measurements (wavenumber range of 780–900 cm^{-1}) were performed using a BRUKER® Senterra with a 532 nm laser source. The electrolyte samples were handled under an argon environment and only exposed to air before the measurement.

3. Results

Figure 1 provides the Raman spectra corresponding to different concentrations of LiTFSI in TG solution. From the figure, the region between 800 cm^{-1} and 900 cm^{-1} can be seen to be characteristic of mixture of modes for ether COC symmetric stretching (v_sCOC) and CH_2 rocking(rCH_2) modes of glymes [18]. The spectral region can be differentiated into two sections: (a) a series of three bands characteristic of various modes of vibration in glymes chains at 809, 828 and 851 cm^{-1}, which in general decreases in intensity as the salt concentration increases, (b) an increase in intensity at a wavenumber if ~873 cm^{-1} with concentration (breathing mode from the complex formation with metal ions; i.e., $M–O_n(A_{1g})$) which refers to more coordinated TG solvent concentration [18,19]. Since the 3 M solution is reported to possess a fully coordinated solvent state [20], the normalization of the solvent coordination peak is performed by considering the boundary conditions (i.e., a zero coordination state in pure solvent and fully coordinated state in 3 M solution) and applying them to the peak intensity at 873 cm^{-1}. Such a similar Raman peak normalization was performed by Tatara et al. [21] in DMSO-based electrolytes. From the normalized data, solvent parameters such as the molar ratio of solvent to salt ([TG]/[LiTFSI]), concentrations of coordinated ($[TG]_{coor}$) and free TG molecules ($[TG]_{free}$) in the electrolyte and coordination number (n) were extrapolated and are shown in Table 1. The solvent parameters for the xM LiTFSI/DMSO electrolytes ($0.05 \leq x \leq 3$) can be found from our previous works [3,4]. It is to be noted that DMSO is a monodentate system where the only available oxygen molecule acts as a solvation centre. This corresponds that for a full solvation of Li^+ ions, ~4 DMSO molecules are involved [3]. However, in case of a multidendate chain molecule such as TG, all the 5 coordination centres are involved in complete solvation of Li^+ ion [20,22].

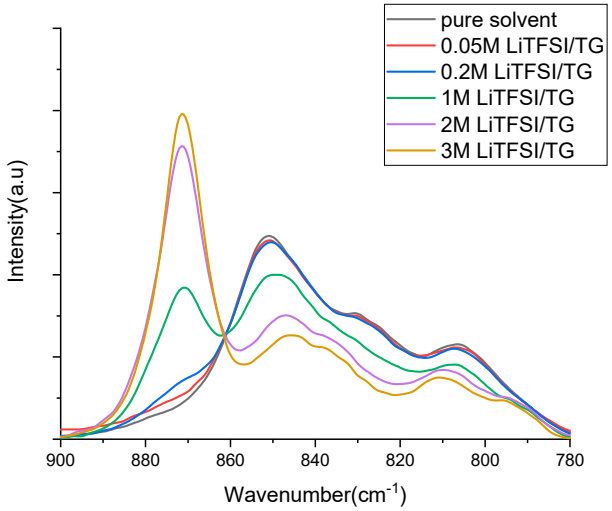

Figure 1. Raman spectra recorded for different concentrated electrolytes of LiTFSI/TG (Tetraglyme).

From the solvent parameters in Table 1, at low concentrations (0.05 M, 0.2 M), the coordination number is found to be in a similar range due to the availability of excess solvent (n [TG]/[LiTFSI] = 87.1 and 21.1 for 0.05 M and 0.2 M respectively). However, the value increases when going from 0.2 M to 1 M and from 1 M to 2 M, unlike in DMSO. Such an increase in coordination number with increasing salt concentration is scarcely reported for TG-based solutions. Recent work by Mandai et.al. suggests that Li^+ transport proceeds via continuous ligand exchange in dilute solution of TG due to the higher solvent/Li^+ ion diffusivity ratio ($D_{sol}/D_{Li}{}^+$) [23]. This leads to a short lifetime of the solvated-cation complex in solutions with excess glymes. In this scenario, the Lewis basicity of anions is higher than, or comparable to, that of the electron-donating group of glymes (ethyl oxide (EO) chain), and the weaker Li^+-EO interaction leads to poor complex formation [24]. In contrast, in concentrated solutions, because of the strong Li^+-solvent interaction, $D_{sol}/D_{Li}{}^+$ approaches unity [23]; i.e., the residence time of solvent increases. This might suggest that Li^+ cations and glymes diffuse together, leading to the formation of a stable $[Li(TG)_n]^+$ complex. As a result of stable complex formation in concentrated electrolytes with increased residence time, Li^+ ions might diffuse with a coordination shell [20]. The effect of co-diffusion in concentrated solutions might be responsible for the increase in coordination number with the increase in salt concentration. In 3 M solution, however, due to the availability of a limited amount of solvent, the coordination number decreases again.

Table 1. Solution properties analyzed from Raman spectra.

Solution	n [TG]/[LiTFSI]	$([TG]_{coor})$ mol/L	$([TG]_{free})$ mol/L	n
Free solvent	-	-	4.53	-
0.05 M LiTFSI/TG	87.14	0.043	4.313	0.81
0.2 M LiTFSI/ TG	21.15	0.152	4.077	0.76
1 M LiTFSI/ TG	3.79	0.995	2.796	0.99
2 M LiTFSI/ TG	1.58	2.217	0.937	1.11
3 M LiTFSI/ TG	0.83	2.502	-	0.83

However, this cannot be the case for DMSO, as the coordination number (n) decreases with the increase in Li-salt concentration. The high DN of DMSO determines the high Li salt dissociation (preferential solvent-separated ion pairs) with the formation of stable Li^+-DMSO complexes. A common example can be deduced from the work of Rocio et al. [25], in which they used Li-containing DMSO:ACN mixtures. They observed the effect of the preferential solvation of Li-salt by DMSO over ACN due to the relative stabilization of ionic species and increased solvent–solute energy coupling

in DMSO-based electrolytes. The relative stabilization of the Li^+-DMSO complex prevents Li^+-anion interaction, affecting the solvent coordination number.

In order to experimentally determine the effect of salt concentration on the Li-redox potential, a concentration cell has been employed. Further information regarding the experimental setup can be obtained from our previous work [4]. Equation (1b) provides the Nernstian potential (E), which is dependent on the activity of Li^+ ($\alpha_{Li}{}^+$) according to Equation (1a) [4].

$$Li^+ + e^- \leftrightarrow Li \tag{1a}$$

$$E = E^\circ + 2.303\frac{RT}{F}\log \alpha_{Li^+} \tag{1b}$$

α_{Li^+} (the activity of lithium species) can be defined as the product of the activity coefficient and concentration of Li^+ species, (γ_{Li^+}) and (C_{Li^+}), respectively; i.e., $\alpha_{Li^+} = C_{Li^+} \times \gamma_{\ Li^+}$. Equation (1b) can be rewritten as

$$E = E^\circ + 2.303\frac{RT}{F}\ (\log \gamma_{Li^+} + \log C_{Li^+}) \tag{2a}$$

Based on our previously published results [4], for Equation (2b), a revised version of the Nernst equation including the concentration (C) of lithium-TG solvated ion complex $Li(TG)_n{}^+$ ($C_{Li[TG]_n{}^+} = C_{Li^+}$) and free TG molecules ($C_{[TG]_{free}}$) is shown in Equation (3).

$$[Li[TG]_n]^+ + e^- \leftrightarrow Li + n[TG]_{free} \tag{2b}$$

$$E = E^\circ + 2.303\frac{RT}{F}log\gamma_{Li^+} + 2.303\frac{RT}{F}log\frac{C_{[Li[TG]_n]^+}}{C_{[[TG]_{free}]^n}} \tag{3}$$

Here, n is the number of TG molecules solvating Li^+. For simplicity, the activity coefficient of Li^+ (γ_{Li^+}) value is assumed to be equal to 1. Measurements using the concentration cell were carried out on five different concentrated solutions ranging from 0.05 M up to 3 M. For all the measurements, the left compartment of the cell was filled with 0.2 M LiTFSI/TG electrolyte, which acted as a measurement reference point. The right compartment was instead filled with the electrolyte under investigation (x= 0.05, 1, 2 and 3 M). The electromotive force (EMF) is therefore described by Equation (4):

$$\mathrm{EMF} E_{Li/Li^+(\ in\ xM)} - E_{Li/Li^+(\ in\ 0.2M)} = 2.303\frac{RT}{F}\left[log\frac{C_{Li(TG)_n{}^+(in\ xM)}}{C_{(TG)_{free}{}^n\ (in\ xM)}} - log\frac{C_{Li(TG)_n{}^+(in\ 0.2M)}}{C_{(TG)_{free}{}^n\ (in\ 0.2M)}}\right] \tag{4}$$

Based on the above equation, the EMF is obtained for all the concentrations and provided in Figure 2. The calculated values are in close agreement with those experimentally measured using the concentration cell. In the case of the 3 M solution, the theoretical EMF between 0.2 and 3 M could not be calculated, as the $C_{(TG)_{free}}$ in the concentrated solution (3 M) is zero (Table 1) and the calculated EMF value in Equation (4) reaches infinity.

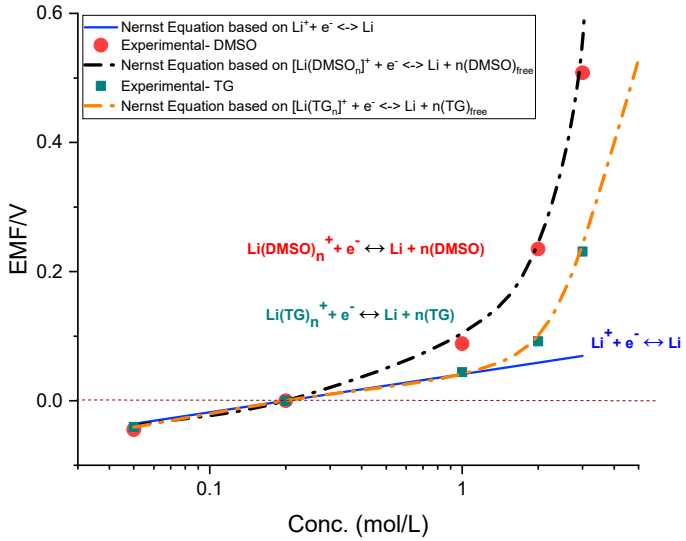

Figure 2. Reference potential measurement compared to the theoretical calculations for different concentrated solutions of DMSO and TG.

Based on our previous knowledge on the use of Fc as a standard internal reference system [4], the measured values of the potential shift in the TG-based solution are further validated using a Fc/Fc^+ redox couple. Figure 3a provides the cyclic voltammogram (CV) measurements of the reversible redox reaction of Fc under varying Li-salt concentrations. In Figure 3a, the x value denotes various concentrations; i.e., 0.2 M, 1 M and 2 M. For this work, a three-compartment beaker cell with a compartment dedicated to the reference electrode is chosen. An Li strip dipped in the electrolyte under investigation in the reference compartment served as the QRE. By eliminating the iR_{ohmic} drop (R_{ohmic} = 767 Ω, 277 Ω and 492 Ω for 0.2 M, 1 M and 2 M, respectively), the peak separation between the oxidation and reduction of Fc was observed to be in the range of 60–64 mV for all the electrolytes under investigation, in agreement with theoretical value of 59 mV for the one-electron reaction [26]. It can be seen that the peak position shifts cathodically as the Li salt concentration in the electrolyte increases. As the Fc/Fc^+ potential is reportedly independent from the salt concentration in the supporting electrolyte, the extent of the observed shift should only depend on the variation of the Li-QRE potential as a function of the salt concentration. The data reported in Figure 2 for the TG electrolytes are therefore used to correct the potential scale of the Fc/Fc^+ CVs. The potential correction for Fc/Fc^+ redox has been made based on Equation (5). Figure 3b shows the CVs for Fc/Fc^+ in all three investigated electrolytes, where the potential is now referred against the Li/Li^+ couple in 0.2 M LiTFSI/TG solution. Moreover, in comparison to our previous work, a notable cathodic shift in Fc/Fc^+ redox potential is observed when the solvent is changed from high-DN DMSO to low-DN TG. As suggested by Calvo et.al [17], assuming the potential of ferrocene is not influenced by the solvent variation due to the small contribution of solvation, such variation arises due to the shift of the Li-QRE potential in each solvent.

$$E_{Fc/Fc^+ corrected} = E_{Fc/Fc^+ measured} + EMF \quad (5)$$

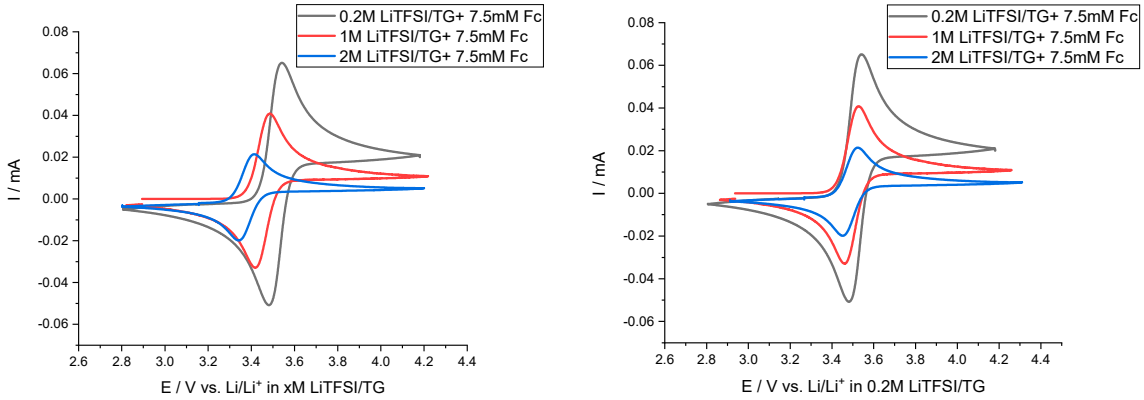

Figure 3. (**a**) Cyclic voltammograms (CVs) recorded for three different concentrations, (**b**) CVs rescaled according to the reference potential of 0.2 M LiTFSI/TG: WE: Au disk, CE/RE: Li strip immersed in the respective electrolyte under study, sweep rate: 10 mV/s. Here, x = 0.2, 1, 2 M.

To understand the effect of the solvent DN on the potential shift trend, we also show in Figure 2 the variation of the EMF of Li| Li symmetrical cells as a function of the Li-salt concentration in DMSO electrolytes [4]. In the case of DMSO, a linear shift in accordance with Equation (1a) is witnessed up to concentration range of 0.2 M. With elevated concentrations, an exponential deviation of Li-QRE is observed [4], which can be explained by considering the solvent activity in Equation (2b). However, in the case of TG, the linear shift of Li-QRE potential extends to 1 M as the exponential deviation can only be witnessed after at higher concentrations. Considering that Equation (1a) is valid only for dilute solutions, in the case of TG, 1 M still acts as a dilute solution. A similar trend is witnessed by Ueno et.al. [18] when the corresponding anion is changed from a highly associated $[OTF]^-$ to a dissociative one $[TFSI]^-$. In the case of an associated salt, due to the strong Li^+-anion interactions (compared to Li^+-solvent interaction) there is a resulting presence of more uncoordinated solvent concentration. This leads in turn to an extended linear shift trend of the Li-redox potential with increased concentration. As discussed above, the weak (Li^+ -solvent) interactions and varied Li^+-solvent complex residence time makes the availability of free solvent in 1 M LiTFSI/TG abundant, thus possibly acting as a dilute solution. Owing to its high DN, a strong Li^+-DMSO interaction exists, which might increase the solvent residence time. The elapsed residence time and possible formation of stable Li^+- $[DMSO]_n$ complex presumably makes the Li^+ ions diffuse in a differentiable way in DMSO in comparison to that in TG solution [27,28].

To understand the effect of the solvent DN on the potential shift trend, we also show in Figure 2 the variation of the EMF of Li| Li symmetrical cells as a function of the Li-salt concentration in DMSO electrolytes [4]. In the case of DMSO, a linear shift in accordance with Equation (1a) is witnessed up to concentration range of 0.2 M. With elevated concentrations, an exponential deviation of Li-QRE is observed [4], which can be explained by considering the solvent activity in Equation (2b). However, in the case of TG, the linear shift of Li-QRE potential extends to 1 M as the exponential deviation can only be witnessed after at higher concentrations. Considering that Equation (1a) is valid only for dilute solutions, in the case of TG, 1 M still acts as a dilute solution. A similar trend is witnessed by Ueno et.al. [18] when the corresponding anion is changed from a highly associated $[OTF]^-$ to a dissociative one $[TFSI]^-$. In the case of an associated salt, due to the strong Li^+-anion interactions (compared to Li^+-solvent interaction) there is a resulting presence of more uncoordinated solvent concentration. This leads in turn to an extended linear shift trend of the Li-redox potential with increased concentration. As discussed above, the weak (Li^+ -solvent) interactions and varied Li^+-solvent complex residence time makes the availability of free solvent in 1 M LiTFSI/TG abundant, thus possibly acting as a dilute

solution. Owing to its high DN, a strong Li^+-DMSO interaction exists, which might increase the solvent residence time. The elapsed residence time and possible formation of stable Li^+- $[DMSO]_n$ complex presumably makes the Li^+ ions diffuse in a differentiable way in DMSO in comparison to that in TG solution [27,28].

4. Conclusions

The effect of the Li-salt concentration on the variation of the Li/Li^+ Quasi-Reference Electrode potential has been investigated. For this work, we chose LiTFSI/TG with five different concentrations (0.05 M, 0.2 M, 1 M, 2 M and 3 M), and a concentration cell was implemented for measurement. Using the revised Nernst equation from our previous knowledge, the potential shift was calculated theoretically, and a good agreement was obtained with the measured values. The obtained values were further validated using an Fc/Fc^+ internal reference couple, which matches with the measured EMF values. One important phenomenon observed is that the onset of deviation in the Li-QRE potential from the trend of the linear (E_{Li/Li^+} vs. log C_{Li^+}) shift in TG was further extended to higher concentration in comparison to that in DMSO-based electrolytes. The increased solvent residence time and formation of a stable solvent- Li^+ complex in DMSO-based solvent owing to its high DN is presumed to be responsible for such a deviation in the potential shift.

Author Contributions: Conceptualization, P.K.R.K., M.M. and M.W.-M.; methodology, P.K.R.K. and M.M.; validation, P.K.R.K., M.M. and S.D.; formal analysis, P.K.R.K.and M.M.; investigation, P.K.R.K.; writing—original draft preparation, P.K.R.K.; writing—review and editing, M.M and S.D.; supervision, S.D., M.W.-M. and M.M.; project administration, M.M.; funding acquisition, M.M. All authors have read and agreed to the published version of the manuscript.

Funding: This research was funded by Bundesministerium für Bildung und Forschung (BMBF) in the framework of LiBaLu project (FKz 03XP0029D).

Acknowledgments: Financial support from Bundesministerium für Bildung und Forschung (BMBF) is gratefully acknowledged.

Conflicts of Interest: The authors declare no conflict of interest.

References

1. Yamada, Y.; Furukawa, K.; Sodeyama, K.; Kikuchi, K.; Yaegashi, M.; Tateyama, Y.; Yamada, A. Unusual stability of acetonitrile-based superconcentrated electrolytes for fast-charging lithium-ion batteries. *J. Am. Chem. Soc.* **2014**, *136*, 5039–5046. [CrossRef] [PubMed]
2. Yamada, Y.; Yamada, A. Review—Superconcentrated Electrolytes for Lithium Batteries. *J. Electrochem. Soc.* **2015**, *162*, A2406–A2423. [CrossRef]
3. Reddy, K.P.K.; Fischer, P.; Marinaro, M.; Wohlfahrt-Mehrens, M. Improved Li-Metal Cycling Performance in High Concentrated Electrolytes for Li-O_2 Batteries. *ChemElectroChem* **2018**, *5*, 1–10.
4. Kottam, P.K.R.; Kalkan, D.; Wohlfahrt-Mehrens, M.; Marinaro, M. Influence of Li-Salt Concentration on Redox Potential of Lithium Metal and Electrochemistry of Ferrocene in DMSO-Based Electrolytes. *J. Electrochem. Soc.* **2019**, *166*, 1574–1579. [CrossRef]
5. Ernould, B.; Sieuw, L.; Barozzino, G.; Gohy, J.; Vlad, A.; Ernould, B.; Sieuw, L.; Barozzino-consiglio, G.; Gohy, J.; Vlad, A. Negative Redox Potential Shift in Fire-Retardant Electrolytes and Consequences for High-Energy Hybrid Batteries. *ACS Appl. Energy Mater.* **2019**, *2*, 11. [CrossRef]
6. Mozhzhukhina, N.; Longinotti, M.P.; Corti, H.R.; Calvo, E.J. Electrochimica Acta A conductivity study of preferential solvation of lithium ion in acetonitrile-dimethyl sulfoxide mixtures. *Electrochim. Acta* **2015**, *154*, 456–461. [CrossRef]
7. Lutz, L.; Yin, W.; Grimaud, A.; Alves Dalla Corte, D.; Tang, M.; Johnson, L.; Azaceta, E.; Sarou-Kanian, V.; Naylor, A.J.; Hamad, S.; et al. High capacity Na-O2 batteries: Key parameters for solution-mediated discharge. *J. Phys. Chem. C* **2016**, *120*, 20068–20076. [CrossRef]
8. Cataldo, F. A revision of the gutmann donor numbers of a series of phosphoramides including tepa. *Eur. Chem. Bull.* **2015**, *4*, 92–97.

9. Bondue, C.J.; Hegemann, M.; Molls, C.; Thome, E.; Baltruschat, H. A Comprehensive Study on Oxygen Reduction and Evolution from Lithium Containing DMSO Based Electrolytes at Gold Electrodes. *J. Electrochem. Soc.* **2016**, *163*, A1765–A1775. [CrossRef]
10. Bondue, C.J.; Reinsberg, P.; Abd-El-Latif, A.A.; Baltruschat, H. Oxygen reduction and oxygen evolution in DMSO based electrolytes: The role of the electrocatalyst. *Phys. Chem. Chem. Phys.* **2015**, *17*, 25593–25606. [CrossRef]
11. Marinaro, M.; Riek, U.; Eswara Moorthy, S.K.; Bernhard, J.; Kaiser, U.; Wohlfahrt-Mehrens, M.; Jörissen, L. Au-coated carbon cathodes for improved oxygen reduction and evolution kinetics in aprotic Li-O2batteries. *Electrochem. Commun.* **2013**, *37*, 53–56. [CrossRef]
12. Marinaro, M.; Theil, S.; Jörissen, L.; Wohlfahrt-Mehrens, M. New insights about the stability of lithiumbis(trifluoromethane) sulfonimide-tetraglyme as electrolyte for Li-O2 batteries. *Electrochim. Acta* **2013**, *108*, 795–800. [CrossRef]
13. Balasubramanian, P.; Marinaro, M.; Theil, S.; Wohlfahrt-Mehrens, M.; Jrissen, L. Au-coated carbon electrodes for aprotic Li-O2 batteries with extended cycle life: The key issue of the Li-ion source. *J. Power Sources* **2015**, *278*, 156–162. [CrossRef]
14. Marinaro, M.; Balasubramanian, P.; Gucciardi, E.; Theil, S.; Joerissen, L.; Wohlfahrt-Mehrens, M. Importance of Reaction Kinetics and Oxygen Crossover in aprotic Li-O-2 Batteries Based on a Dimethyl Sulfoxide Electrolyte. *ChemSusChem* **2015**, *8*, 3139–3145. [CrossRef]
15. Jung, H.G.; Hassoun, J.; Park, J.B.; Sun, Y.K.; Scrosati, B. An improved high-performance lithium-air battery. *Nat. Chem.* **2012**, *4*, 579–585. [CrossRef]
16. Peng, Z.; Freunberger, S.A.; Chen, Y.; Bruce, P.G. A reversible and higher-rate Li-O2 battery. *Science* **2012**, *337*, 563–566. [CrossRef]
17. Mozhzhukhina, N.; Calvo, E.J. The Correct Assessment of Standard Potentials of Reference Electrodes in Non-Aqueous Solution. *J. Electrochem. Soc.* **2017**, *164*, 2295–2297. [CrossRef]
18. Ueno, K.; Tatara, R.; Tsuzuki, S.; Saito, S.; Doi, H.; Yoshida, K.; Mandai, T.; Matsugami, M.; Umebayashi, Y.; Dokk, K.; et al. Li+ solvation in glyme–Li salt solvate ionic liquids. *Phys. Chem. Chem. Phys.* **2015**, *17*, 8248–8257. [CrossRef]
19. Brouillette, D.; Irish, D.E.; Taylor, N.J.; Perron, G.; Odziemkowski, M.; Desnoyers, J.E. Stable solvates in solution of lithium bis(trifluoromethylsulfone)imide in glymes and other aprotic solvents: Phase diagrams, crystallography and Raman spectroscopy. *Phys. Chem. Chem. Phys.* **2002**, *4*, 6063–6071. [CrossRef]
20. Tsuzuki, S.; Shinoda, W.; Matsugami, M.; Umebayashi, Y.; Ueno, K.; Mandai, T.; Seki, S.; Dokko, K.; Watanabe, M. interactions with anions in equimolar mixtures of glymes and Li [TFSA]: Analysis by molecular dynamics simulations †. *Phys. Chem. Chem. Phys.* **2014**, *17*, 126–129. [CrossRef] [PubMed]
21. Tatara, R.; Kwabi, D.G.; Batcho, T.P.; Tulodziecki, M.; Watanabe, K.; Kwon, H.M.; Thomas, M.L.; Ueno, K.; Thompson, C.V.; Dokko, K.; et al. Oxygen Reduction Reaction in Highly Concentrated Electrolyte Solutions of Lithium Bis(trifluoromethanesulfonyl)amide/Dimethyl Sulfoxide. *J. Phys. Chem. C* **2017**, *121*, 9162–9172. [CrossRef]
22. Sun, Y.; Hamada, I. Insight into the Solvation Structure of Tetraglyme-Based Electrolytes via First-Principles Molecular Dynamics Simulation. *J. Phys. Chem. B* **2018**, *122*, 10014–10022. [CrossRef] [PubMed]
23. Mandai, T.; Yoshida, K.; Ueno, K. Criteria for solvate ionic liquids †. *Phys. Chem. Chem. Phys.* **2014**, *16*, 8761–8772. [CrossRef] [PubMed]
24. Ueno, K.; Yoshida, K.; Tsuchiya, M.; Tachikawa, N.; Dokko, K.; Watanabe, M. Glyme—Lithium Salt Equimolar Molten Mixtures: Concentrated Solutions or Solvate Ionic Liquids? *J. Phys. Chem. B* **2012**, *116*, 11323. [CrossRef] [PubMed]
25. Semino, R.; Zaldívar, G.; Calvo, E.J.; Laria, D.; Semino, R.; Zaldívar, G.; Calvo, E.J.; Laria, D. Lithium solvation in dimethyl sulfoxide-acetonitrile mixtures Lithium solvation in dimethyl sulfoxide-acetonitrile mixtures. *J. Chem. Phys.* **2014**, *141*, 214509. [CrossRef] [PubMed]
26. Laoire, C.O.; Plichta, E.; Hendrickson, M.; Mukerjee, S.; Abraham, K.M. Electrochimica Acta Electrochemical studies of ferrocene in a lithium ion conducting organic carbonate electrolyte. *Electrochim. Acta* **2009**, *54*, 6560–6564. [CrossRef]

27. Li, Z.; Borodin, O.; Smith, G.D.; Bedrov, D. Effect of Organic Solvents on Li+ Ion Solvation and Transport in Ionic Liquid Electrolytes: A Molecular Dynamics Simulation Study. *J. Phys. Chem. B* **2015**, *119*, 3085–3096. [CrossRef]
28. Borodin, O.; Smith, G.D. Li + Transport Mechanism in Oligo (Ethylene Oxide) s Compared to Carbonates. *J. Solut. Chem.* **2007**, *36*, 803–813. [CrossRef]